Journal of Achievements in Materials and Manufacturing Engineering
VOLUME 24
ISSUE 2
October
2007

The impact of production methods on the properties of gradient tool materials

L.A. Dobrzański [a,*], A. Kloc-Ptaszna [a], G. Matula [a], J.M. Contreras [b], J.M. Torralba [b]
[a] Division of Materials Processing Technology, Management and Computer Techniques in Materials Science, Institute of Engineering Materials and Biomaterials, Silesian University of Technology, ul. Konarskiego 18a, 44-100 Gliwice, Poland
[b] Universidad Carlos III de Madrid, Avda. Universidad, 30.E-28911 Leganés, Spain
* Corresponding author: E-mail leszek.dobrzanski@polsl.pl

Received 30.03.2007; published in revised form 01.10.2007

Materials

ABSTRACT

Purpose: The goal of this work is to obtain the gradient materials based on the non-alloyed steel reinforced high-speed steel using the conventional powder metallurgy method and pressureless forming powder metallurgy.
Design/methodology/approach: Forming methods were developed during the investigations for high-speed and unalloyed steel powders, making it possible to obtain materials with six layers in their structure. The non-alloyed steel was fabricated by mixing iron powders with graphite.
Findings: It was found out, basing on the hardness tests, that the layer built of steel without any alloy elements demonstrates very low hardness in comparison with the transition layer and the HS6-5-2 high-speed layer. The density of the specimens rises with increasing temperature. It was also observed that porosity decreases along with the carbon content in these layers.
Practical implications: It was noticed, that increase of the sintering temperature results in the uncontrolled growth and coagulation of the primary carbides and melting up to forming of eutectics in layers consisting of the high-speed steel. Developed material is tested for turning tools.
Originality/value: The layers were poured in such way that the first layers consisted of the non-alloy steel and the last one from the high-speed steel, and were compacted next. The layers inside the material are mixes of the high-speed steel and non-alloy steel powders in the relevant proportions.
Keywords: Gradient tool materials; Powder metallurgy; High-speed steel; Non-alloyed steel

1. Introduction

Functionally gradient materials (FGM) are materials whose properties change in their volume. The property gradient in the material is caused by a position-dependent chemical composition, microstructure or atomic order. The material properties can change continuously, gradually or discreetly (abruptly). Gradation processes can be classified into constitutive, homogenizing and segregating processes. Constitutive processes are based on a stepwise build-up of the graded structure from precursor materials or powders. In homogenizing processes a sharp interface between two materials is converted into a gradient by material transport. Segregating processes start with a macroscopically homogeneous material which is converted into a graded material by material transport caused by an external field. Homogenizing and segregating processes produce continuous gradients, but have limitations concerning the types of gradients which can be produced [1-10].

For several decades there have been attempts to develop and produce a tool material which would demonstrate high abrasion resistance in use coupled with high ductility. In reality combining such properties is impossible to achieve. Nonetheless, various attempts to partially solve this problem by creating layer structures, developing composite materials, applying single-layer PVD and CVD coatings, pad welding or spraying hard layers with the metal spraying method, have been undertaking. The above methods, however, demonstrate several disadvantages including all kinds of limitations connected with inappropriate surface layer thickness, adhesion of the surface layer, or excessive stress between the surface layers and the base. Due to these limitations, research work is continued to develop technologies which would lead to obtaining functionally gradient materials (FGM) and applying gradient surface coatings composed of various tool materials, i.e. high-speed steels, tool alloy steels for hot-work and cold-work applications, onto appropriate base materials. The use of the powder metallurgy method offers a combination of high abrasion resistance (characteristic of sintered carbides and cermetals), high ductility (corresponding to high-speed steels and traditional carbide-steels) and lower production costs. The main advantage of these materials is extremely high abrasion resistance combined with relatively high ductility of the core material, which is particularly important in materials designed for die tools, hot-work plastic forming tools, heavy duty machining tools for high-speed operation and shape machining tools. The main objective of this work is to develop modern gradient materials through the powder metallurgy methods in order to ensure the required properties and structure of the designed material [11-15].

2. Materials for research

The experiments were carried out on specimens produced using the pressureless forming method, the conventional powder metallurgy method involving powder compacting in the closed matrix followed by sintering, and the cold isostatic pressing method. The powders used for specimen production are detailed in Table 1. The particles of the gas- and water-atomized HS6-5-2 high-speed steel powders, as well as iron and carbon particles are shown in fig. 1. The chemical composition of the gas- and water-atomized HS6-5-2 high-speed steel powder is shown in Table 2.

Table 1.
Powders used for fabricating the materials

Powder	Grain size, µm	Additional information
HS6-5-2	>21	High-speed steel powder, gas atomized, from OSPREY METALS, Neath, UK
HS6-5-2	>150	High-speed steel powder, water atomized, from HOGANAS
Fe	>50	from Eckagranules, Senecorut, F-60140 Baileval
C	99.5%<40 50%<18	Natural, layered coal, class EDM96-97, ISMAF

a)

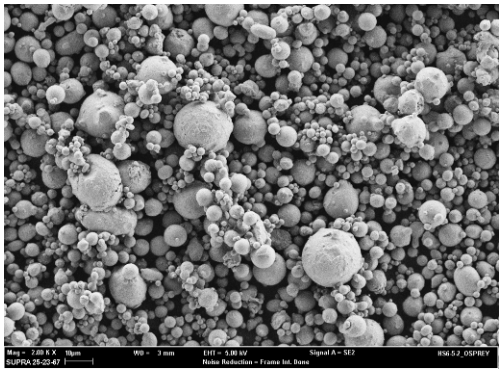

b)

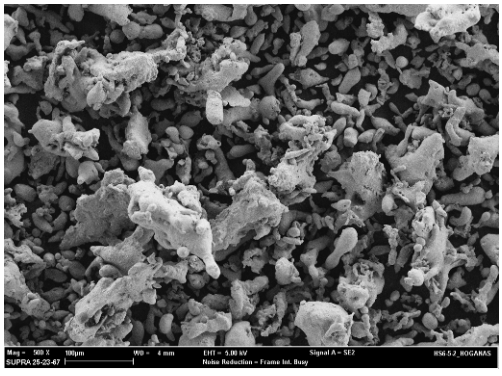

c)

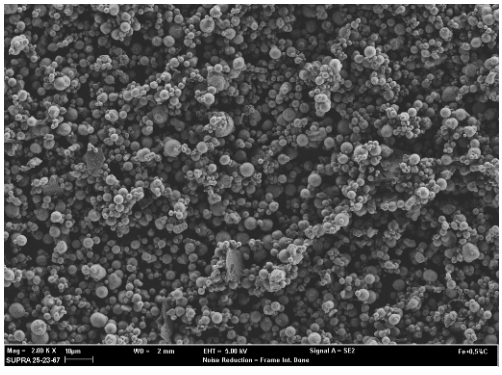

d)

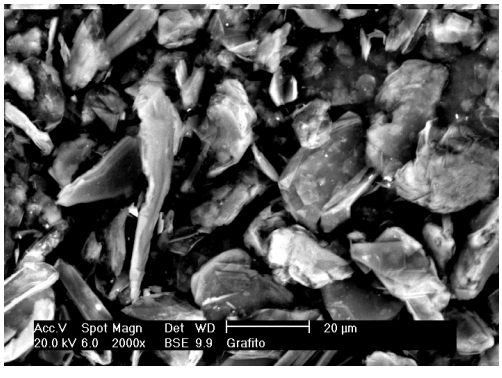

Fig. 1. Scanning electron micrographs of: a) HS6-5-2, gas atomized, b) HS6-5-2 water atomized, c) iron, d) carbon powders

Table 2.
Chemical composition of Osprey and Hoganas HS6-5-2 high-speed steel powders

Element	Mass concentration, [%]	
	Osprey	Hoganas
C	0,82-0,92	0,75-0,90
Mn	≤0,4	0,20-0,45
Si	≤0,5	≤0,45
P	≤0,030	≤0,04
S	≤0,030	≤0,04
Cr	3,5-4,5	3,75-4,5
Ni	≤0,4	0,2
Mo	4,5-5,5	4,5-5,5
W	6,0-7,0	5,50-6,75
V	1,7-2,1	1,6-2,2
Co	≤0,5	0,1
Cu	≤0,3	0,1
Fe	rest	rest

The uniaxially pressed and sintered specimens were made from the HS6-5-2-Hoganas powder (due to its better charge density compared to the M2-Osprey) and the unalloyed steel powder. The pressing was carried out in an uniaxial, single-action die (fig. 2a). The powder was put in a die placed between two punches: one stationary and one moving. The pressing was carried out at the pressure of 500MPa.

The specimens obtained through isostatic pressing and sintering were made from the HS6-5-2-Hoganas, the HS6-5-2-Osprey and the unalloyed steel powders. The pressing of the powder is performed at ambient temperature, under pressure transferred by the liquid. The powder filled form (placed in a special container) was immersed in a liquid pressing medium exerting even pressure on the surface of the initially formed specimen (fig. 2b) [11].

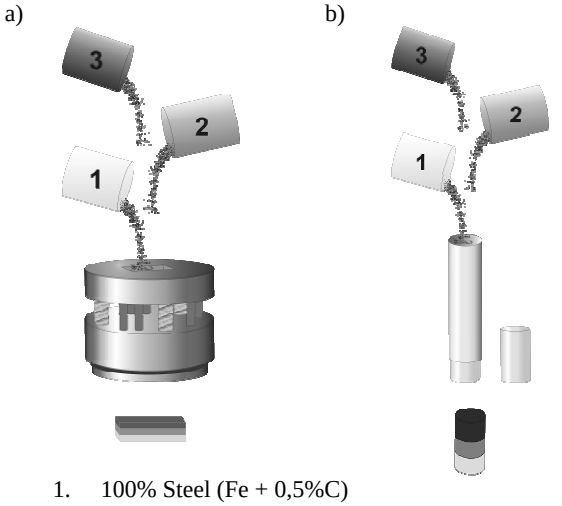

1. 100% Steel (Fe + 0,5%C)
2. 50% Steel (Fe +0,5%C) + 50% HS6-5-2
3. 100% HS6-5-2

Fig. 2. Powder forming sequence and proportions for uniaxially pressed and isostatic pressing

The pressureless powder forming, uniaxial pressing and cold isostatic pressing methods were used to make the profiles. The pressureless powder forming method consists in mixing the binding agent with metal powders, the Loctite PMS 90E thermo-setting resin was used as the binding agent (liquid in ambient temperature and polymerizing in the 80÷90^{o}C temperature range). The binding agent density was 1.0 g/cm^{3}. The following powders were used for making the greens: HS6-5-2-Osprey and the unalloyed steel powder. The metal powder volume fraction was 60% [11-15].

Next, the layers of the polymer/powder slurry were poured into glass moulds and were respectively subjected to polymerization, starting from the slurry which did not contain high-speed steel. The binding agent polymerization process was performed in an electric, chamber furnace at the temperature 90^{o}C over the period of 15 minutes. The polymer/powder profiles thus obtained were removed from the glass moulds (fig. 3) and subjected to thermal binding agent degradation in a chamber furnace at the temperature of 400-550^{o}C in steps of 50^{o}C in the atmosphere of the flowing argon N2-10%H2. Carbon concentration analysis, depending on the binding agent degradation and sintering temperatures, was carried out with the LECO CS-200 type apparatus [11-15].

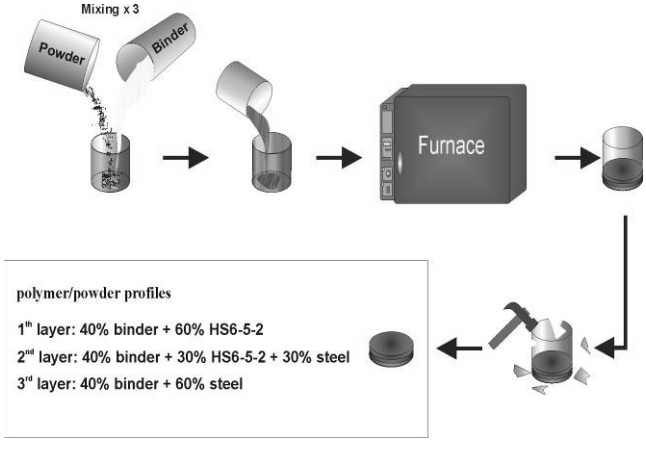

Fig. 3. Metal powder and binding agent fraction

The sintering was carried out in a vacuum furnace at the temperature 1100÷1350^{o}C in steps of 50^{o}C. In order to prevent cracking the specimens were heated at the rate of not exceeding 5^{o}C/min.

All the specimens in the sintered state, obtained through various powder forming methods, were then subjected to density, hardness and porosity testing, and were observed on a scanning electron microscope (SEM) additionally furnished with a backscattered electron detector and energy dispersive analyzer (EDAX D4). The density testing was performed with the Archimedes method consisting in measuring the specimen virtual mass immersed in water. Hardness was measured using the Vickers hardness tester with the intender load of 9.8N. The measurements were taken across the whole width of the sample section with seven measurement points for each layer. The porosity testing was carried out using an optical microscope. For each measurement 5 random points were selected from each layer [11-15].

3. Results and discussion

Basing on the thermogravimetric examination the binding agent thermal degradation cycle was selected for the specimens with thermosetting resin (fig. 4). The degradation cycle was selected to include three isothermic stops lasting 30 minutes each. The first stop starts at the initial degradation temperature, i.e. 200°C, the next one at 300°C, and the third at 400, 450 or 500°C. The heating rate from ambient temperature to the first isothermic stop, and from the first to the second isothermic stop was selected experimentally at 1°C/min. Between the first and the second isothermic stop the heating rate is 2°C/min. After the completion of the binding agent degradation cycle, cooling down to ambient temperature. The cooling rate is 5°C/min. The heating and cooling rates were selected to prevent cracking caused by increasing gas pressure inside the forming pores [11-15].

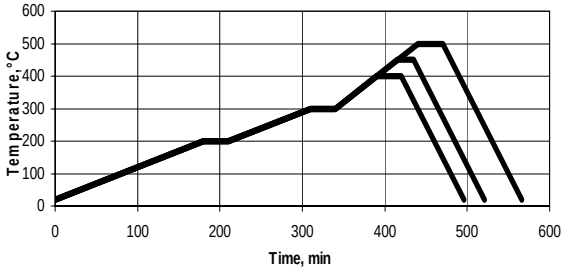

Fig. 4. The degradation of the binding agent cycle

The specimens made with the pressureless forming method were found to contain the highest carbon concentration after degradation at 350°C (fig. 5). Carbon concentration depends on the binding agent degradation temperature, the green arrangement in the furnace and on the flow direction of the gas used.

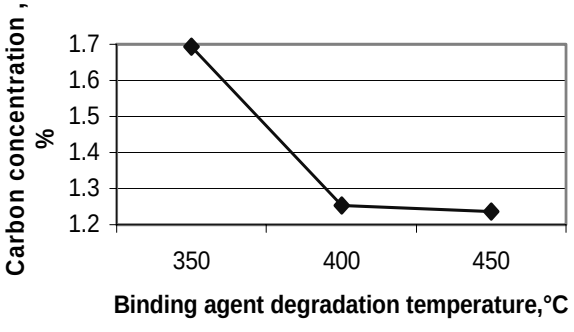

Fig. 5. The impact of the binding agent degradation temperature on carbon concentration in pressurelessly formed specimens

The hardness of all the specimens obtained through pressureless forming as well as compacting and sintering rises with the higher sintering temperature (fig. 6). The layer built of steel without any alloy elements demonstrates very low hardness in comparison with the transition layer and the HS6-5-2 high-speed layer. The highest hardness is demonstrated by the specimens following the cold isostatic pressing made from the Osprey high-speed steel powder.

The density of the specimens subjected to thermal debinding and sintered at 1150, 1250 or 1350°C depends on the sintering temperature. The density rises with increasing temperature. The density examination results for pressurelessly formed steels (PLF) and compacted and sintered steels (PM) are shown in fig. 7.

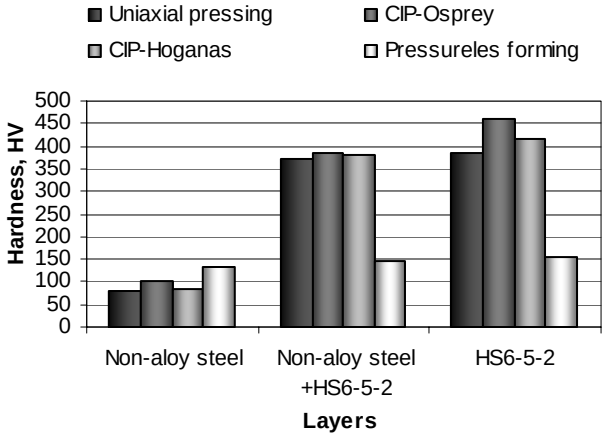

Fig. 6. Mean hardness values (for three layers) for PLF and PM specimens

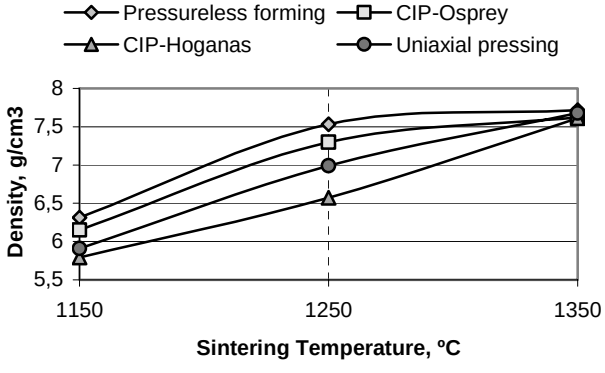

Fig. 7. The density/sintering temperature chart for PLF and PM specimens

Irrespectively of the production method, for the specimens compacted and sintered at the temperature of 1250°C, three gradually changing layers in the material volume are observed (fig. 8). The pores visible in the unalloyed steel layers indicate an incomplete sintering process. These pores disappear when the sintering temperature is increased. The pores are smaller in the high-speed and transition layers at the temperature exceeding 1250°C. Mean porosity values are shown in fig. 9. Basing on the microstructure examination it was found that the sintering temperature which ensures high density and homogeneous structure with fine primary carbide precipitations, should not exceed 1250°C.

a)

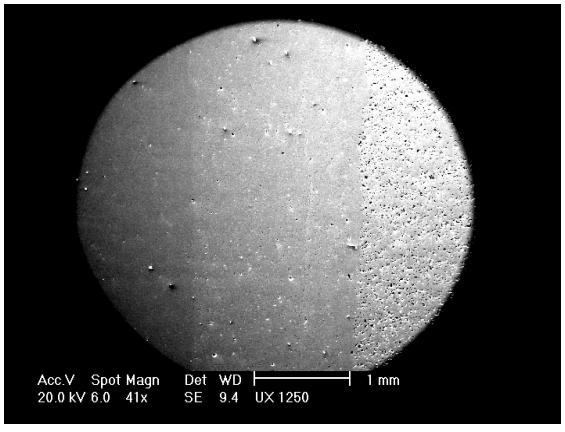

b)

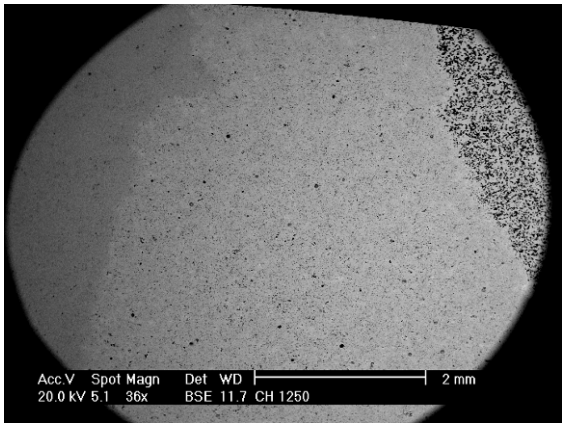

c)

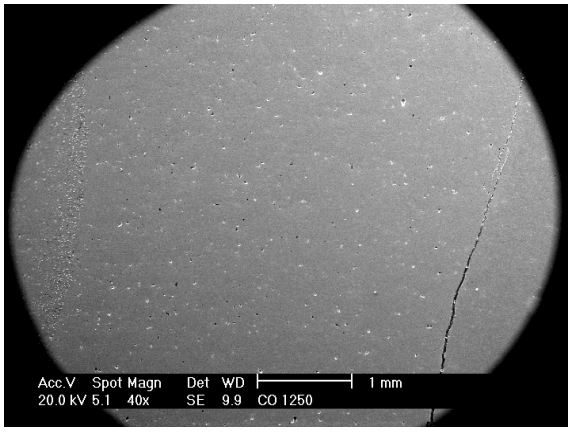

Fig. 8. The structure of specimens sintered at the temperature of 1250°C: a) after uniaxial pressing, b) after cold isostatic pressing using the Hoganas powder, c) after cold isostatic pressing using the Osprey powder

In the case of the compacted and sintered specimens the sintering temperature should be about 1300°C (fig. 12). It was noted that irrespective of the method the increasing sintering temperature in the high-speed steel layers causes uncontrollable growth and coagulation of primary carbides. Basing on the structure examination of the pressurelessly formed as well as compacted and sintered specimens the high-speed and transition layers were found to contain finely distributed carbides. As a result of the increase in the sintering temperature, carbide coagulation and melting leading to eutectic formation occur. (fig. 13).

a)

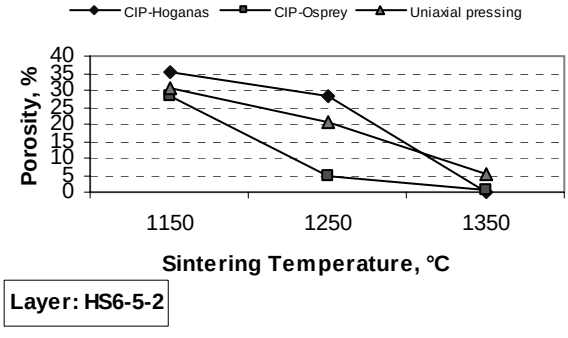

Layer: HS6-5-2

b)

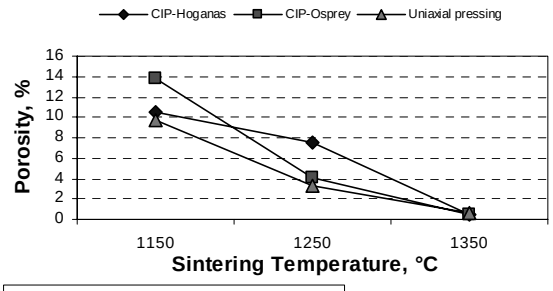

Layer: HS6-5-2 + unalloyed steel

c)

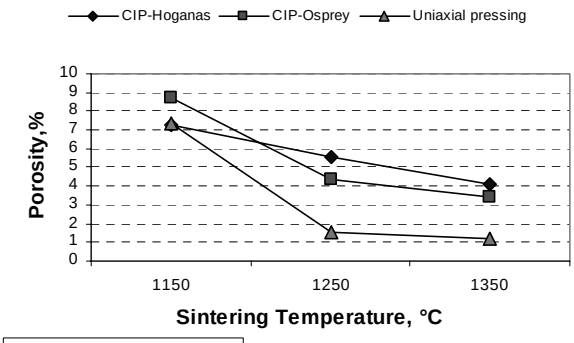

Layer: unalloyed steel

Fig. 9. Porosity comparison for compacted and sintered specimens: a) HS6-5-2 high-speed steel layer, b) transition layer (50% HS6-5-2 high-speed steel and 50% unalloyed steel), c) unalloyed steel layer

Basing on the microstructure examination it was found that the sintering temperature which ensures high density and homogeneous structure with fine primary carbide precipitations, should not exceed 1250°C .

For the pressurelessly formed specimens, the high-speed and transition layers were found to contain finely distributed carbides. As a result of the increase in the sintering temperature, carbide coagulation and melting leading to eutectic formation occur (fig.10).

a)

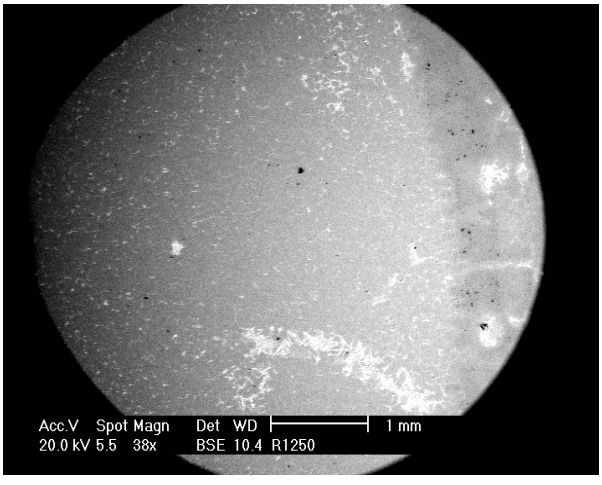

b)

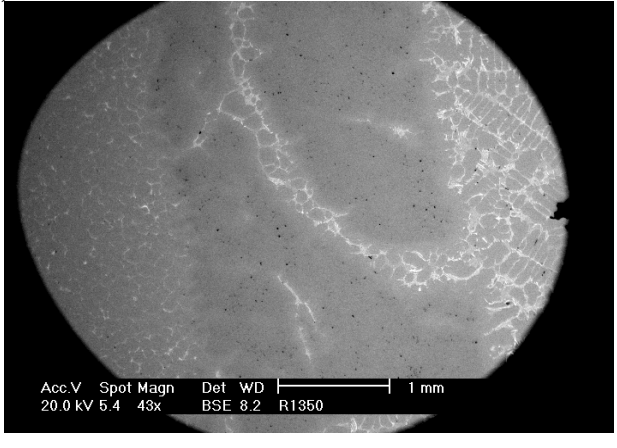

Fig. 10. The structure of specimens made with pressureless forming and sintered at the temperature of: a) 1250°C, b) 1350°C

It was found out basing on investigations of the fabricated materials that the portion of pores in the particular layers of the gradient materials decreases along with the carbon concentration increase in particular layers. An increase of carbon concentration lowers the sintering temperature in all layers. Therefore, five test pieces were made with varying carbon content to select the optimum value of carbon concentration and sintering temperature. The way in which the powder slurry is poured was also modified (fig.11).

Microhardness of the compacted and sintered test pieces grows along with the carbon concentration and sintering temperature increase. The layer from steel without any addition of alloying elements demonstrates very low hardness compared to the intermediate layers and the layer from the HS6-5-2 high-speed steel (fig. 12).

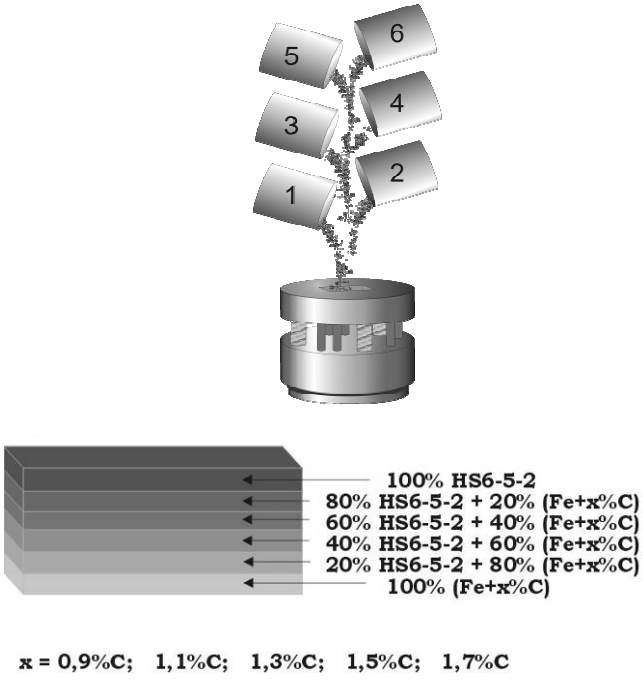

Fig. 11. Powder forming sequence and proportions uniaxially pressed

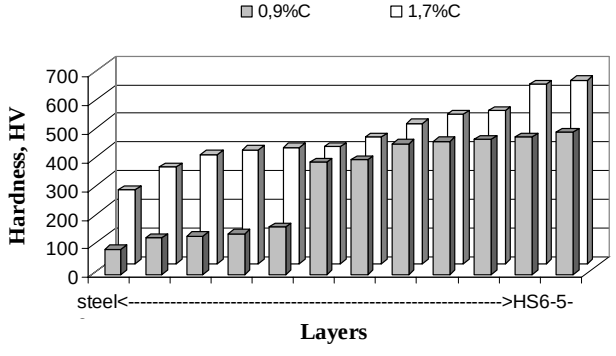

Fig. 12. Mean hardness values (for six layers) for PM specimens

In case of test pieces with a bigger number of layers the boundaries between layers disappear as the carbon concentration grows in the particular layers (fig. 13 a, b, c). In case of materials with the highest carbon content (1.7%) boundaries between the layers are no longer visible. The visible pores in layers with the non-alloy steel indicate to the incomplete sintering process. The pores disappear along with the sintering temperature and carbon content growth in the particular layers.

a)

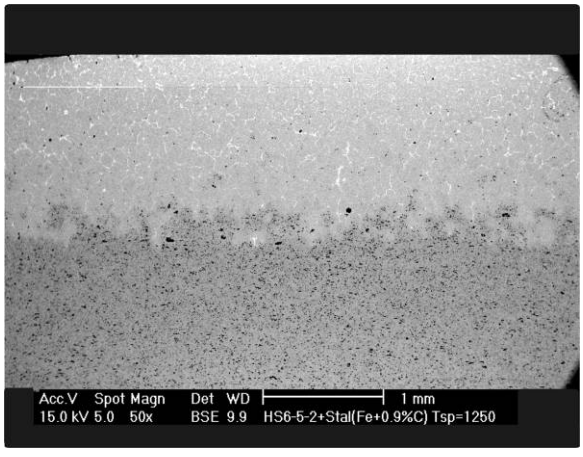

b)

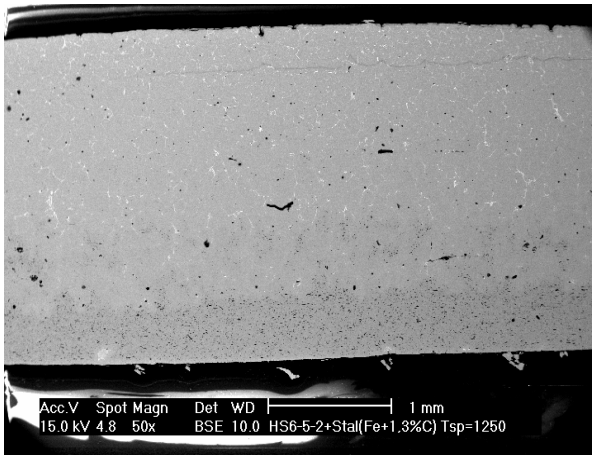

c)

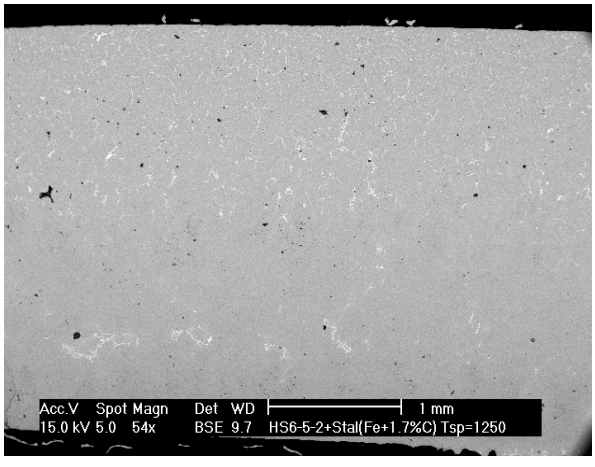

Fig. 13. The structure of specimens sintered at the temperature of 1250°C after uniaxial pressing, with six layers in their structure with deferent carbon concentration values: a) steel (Fe+ 0,9%C), b) steel (Fe+ 1,3%C), c) steel (Fe+ 1,7%C)

4. Summary

Basing on the experimental examination of gradient materials produced through the pressureless forming, uniaxial, single-action pressing and cold isostatic pressing methods, it was found that the materials made with cold pressureless forming demonstrate the highest density reaching about 98% of theoretical density. The pressureless forming method is more viable economically. Apart form the furnace for binding agent degradation and sintering no other equipment is required. Another advantage of this method is the possibility of obtaining a profile of higher density and homogeneous powder distribution in the binding agent matrix. Higher high-speed steel density in pressurelessly formed materials, in comparison with the high-speed steel density in compacted and sintered materials, is caused by higher carbon concentration. The carbon, being a product of binding agent degradation, surrounds the high-speed steel powder grains and, by diffusing into the layers of surface grains, lowers the sintering temperature and initiates the sintering process [10-15]. Hence the sintering temperature corresponding to the maximum density of the pressurelessly formed materials is lower in comparison with the materials made using traditional powder metallurgy methods. In case of the test pieces sintered at temperature of 1250°C - with three layers - one may observe three layers changing gradually (in the material volume). In case of test pieces with a bigger number of layers the boundaries between layers disappear as the carbon concentration grows in the particular layers. In case of materials with the highest carbon content (1.7%) boundaries between the layers are no longer visible. The pores disappear along with the sintering temperature and carbon content growth in the particular layers.

Acknowledgements

Experimental research carried out as part of the Socrates-Erasmus Programme at the Carlos III University in Madrid. SA research carried out as part of the project financed by Scientific Research Committee (KBN), grant no PBZ-KBN-100/T08/2003

References

[1] K. Ichikawa, Functionally Graded Materials in the 21st Centary A Workshop on Trends and Forecasts, Kluwer Academic Publishers 2001.
[2] B. Kieback, A. Neubrand, H. Riedel, Processing techniques for functionally graded materiale, Materials Science and Engineering 362 (2003) 81-106.
[3] M.B. Bever, P.F. Duwez, Gradients in composite materials, Materials Science and Engineering 10 (1972) 1-8.
[4] J. Wessel, The Handbook of Advanced Materials, Enabling New Designs, Materials Technology Series 2004.
[5] L. Jaworska, M. Rozmus, B. Królikowska, A. Twardowska, Functionally gradem cermets, Journal of Achievements in Materials and Manufacturing Engineering 17 (2006) 73-76.
[6] Y. Miyamoto, W.A. Kaysser, B.H. Rabin, A. Kawasaki, R.G. Ford, Functionally Graded Materials, Design, Processing and Applications, Kluwer Academic Publishers, Boston-Dordrecht-London, 1999.
[7] W. Lengauer, K. Dreyer, Functionally graded hardmetals, Journal of Alloys and Compounds 338 (2002) 194-212.

[8] S. Suresh, A. Mortensen, Fundamentals of functionally graded materials, IOM Communications Limited, London, 1999.
[9] A. Salak, M. Selecká, H. Danninger, Machinability of Powder Metallurgy Steels, Cambridge Iinternational Science Publishing, 2005.
[10] C. Klingshirn, M. Koizumi; F. Haupert, H. Giertzsch,; K. Friedrich, Structure and wear of centrifuged epoxy-resin/carbon fiber functionally graded materials, Journal of Materials Science Letters, 19 (2000) 263-266.
[11] L.A. Dobrzański, A. Kloc, G. Matula, J.M. Contreras, J.M. Torralba, The impact of production methods on the structure and properties of gradient tool materials of unalloyed steel matrix reinforced with HS6-5-2 high-speed steel, Proceedings of the 11th International Scientific Conference on the Contemporary "Achievements in Mechanics, Manufacturing and Materials Science" CAM3S'2005, Gliwice-Zakopane, 223-229 (CD-ROM).
[12] L.A. Dobrzański, A. Kloc, G. Matula, J. Domagała, J.M. Torralba, Effect of carbon concentration on structure and properties of the gradient tool materials, Journal of Achievements in Materials and Manufacturing Engineering 17 (2006) 45-48.
[13] L.A. Dobrzański, A. Kloc-Ptaszna, A. Dybowska, G. Matula, E. Gordo J.M. Torralba, Effect of WC concentration on structure and properties of the gradient tool materials, Journal of Achievements in Materials and Manufacturing Engineering 20 (2007) 91-94.
[14] A. Kloc, L.A. Dobrzański, G. Matula, J.M. Torralba, Effect of manufacturing methods on structure and properties of the gradient tool materials with the non-alloy steel matrix reinforced with the HS6-5-2 type high-speed steel, International Conference on Processing and Manufacturing of Advanced Materials, Processing, Fabrication, Properties, Applications THERMEC' 2006, Vancouver- Canada, 2749-2754 (CD-ROM).
[15] L.A. Dobrzański, A. Kloc-Ptaszna, G. Matula, J.M. Torralba, Structure and properties of the gradient tool materials of unalloyed steel matrix reinforced with HS6-5-2 high-speed steel, Archives of Materials Science and Engineering 28 (2007) 197-202.